ENVIRONMENTAL RESEARCH LETTERS

LETTER • OPEN ACCESS

Modulation of the impact of winter-mean warm Arctic-cold Eurasia pattern on Eurasian cold extremes by the subseasonal variability

To cite this article: Sai Wang *et al* 2024 *Environ. Res. Lett.* **19** 034043

ENVIRONMENTAL RESEARCH
LETTERS

CrossMark

OPEN ACCESS

RECEIVED
28 September 2023

REVISED
19 February 2024

ACCEPTED FOR PUBLICATION
23 February 2024

PUBLISHED
5 March 2024

LETTER

Modulation of the impact of winter-mean warm Arctic-cold Eurasia pattern on Eurasian cold extremes by the subseasonal variability

Sai Wang[1,*], Minghu Ding[1], Guancheng Li[2] and Wen Chen[3]

[1] State Key Laboratory of Severe Weather, Chinese Academy of Meteorological Sciences, Beijing 100081, People's Republic of China
[2] Eco-Environmental Monitoring and Research Center, Pearl River Valley and South China Sea Ecology and Environment Administration, Ministry of Ecology and Environment, PRC, Guangzhou 510611, People's Republic of China
[3] Department of Atmospheric Sciences, Yunnan University, Kunming 650500, People's Republic of China
[*] Author to whom any correspondence should be addressed.

E-mail: wangs@cma.gov.cn

Keywords: WACE pattern, sub-seasonal variability, cold extremes, Ural-Siberian blocking

Supplementary material for this article is available online

Abstract

Utilizing ERA5 data, this study provides evidence that both the winter-mean state and subseasonal variability (SSV) of the warm Arctic-cold Eurasia (WACE) pattern significantly influence the frequency of cold extremes in Eurasia. The positive phase of winter-mean WACE ($\text{WACE}_{\text{Mean}}$) or a stronger SSV of WACE (WACE_{SSV}) corresponds to a higher occurrence of cold extremes over central Eurasia and East Asia. Furthermore, the study reveals that the impact of $\text{WACE}_{\text{Mean}}$ on the cold extremes is modulated by WACE_{SSV}. During years characterized by a positive $\text{WACE}_{\text{Mean}}$ and enhanced WACE_{SSV}, the associated winter-mean anticyclonic anomalies, combined with amplified subseasonal circulation fluctuations over the northern Eurasia continent, contribute to a significant increase in the blocking frequency over the Ural–Siberia region. This, in turn, contributes to an intensified occurrence of cold extremes in central Eurasia and East Asia. In contrast, during the years with a positive $\text{WACE}_{\text{Mean}}$ but reduced WACE_{SSV}, in the absence of significant changes in the subseasonal circulation fluctuations, the winter-mean anticyclonic anomalies over the northern Eurasia continent do not exert a significant impact on Ural–Siberian blocking frequency by themselves. Consequently, there are no notable anomalies in the frequency of cold extremes over central Eurasia and East Asia. Finally, this study reveals that the differences in the distribution of the frequency anomalies in the blocking between the two sets of years are attributed to the constructive and destructive superposition of anomalies in subseasonal circulation fluctuations related to the $\text{WACE}_{\text{Mean}}$ and WACE_{SSV}.

1. Introduction

Global warming has been suggested to alter the probabilities of temperature extremes occurring worldwide, leading to increased heatwaves and decreased cold waves (Stott *et al* 2004, Alexander *et al* 2006, Peterson *et al* 2012, Schoetter *et al* 2015, Screen *et al* 2015, Herring *et al* 2016). However, from the late 1980s through the early 2010s, the Northern Hemisphere mid-latitudes, particularly Eurasia region, have experienced a cooling trend and an increase in high-impact cold extremes despite ongoing global temperature rise (Overland *et al* 2011, Cohen *et al* 2012, Zhang *et al* 2012, Johnson *et al* 2018). In densely populated East Asia, the extreme cold events have not only become more frequent but also stronger and longer-lasting (Woo *et al* 2012, Tang *et al* 2013, Sun *et al* 2016), causing significant disruptions to economies and societies in the region (Gong *et al* 2014, Wu *et al* 2017).

The cooling anomalies observed over Eurasia region are closely linked to pronounced warming anomalies in the Arctic, forming a distinct pattern known as the 'warm Arctic-cold Eurasia' (WACE) pattern (Overland *et al* 2011, Cohen *et al* 2014). Since the mid-2000s, the winter-mean WACE pattern ($\text{WACE}_{\text{Mean}}$) has consistently shown a persistent positive phase, contributing significantly to the increased occurrence of severe winters in Eurasia (Mori *et al* 2014, Wang *et al* 2020b). However, there is ongoing debate regarding whether the changes in the magnitude and polarity of the $WACE_{Mean}$ can be attributed to Arctic sea ice loss (Blackport and Screen 2020, Cohen *et al* 2020, Zappa *et al* 2021). Some studies suggest that Arctic sea ice loss contributes to the changes observed in the $WACE_{Mean}$ (Wu *et al* 2011, 2015, 2022, Mori *et al* 2014, 2019, Outten *et al* 2023). Specifically, the background conditions associated recent rapid loss of Arctic sea ice and subsequent rapid Arctic warming favor the more frequent occurrence of Ural blocking highs and intensified Siberian highs, leading to increased occurrence of severe winters (Honda *et al* 2009, Liu *et al* 2012, Cohen *et al* 2014, Mori *et al* 2014, 2019, Yao *et al* 2017). However, a significant number of studies based on models have questioned the impact of sea ice on the $WACE_{Mean}$ (Sun *et al* 2016, Blackport and Screen 2021, Komatsu *et al* 2022). These studies have found little impact of sea ice on midlatitude variability and multidecadal trends during winter (Ogawa *et al* 2018, Koenigk *et al* 2019), or they have detected midlatitude responses to sea ice loss that are much weaker compared to internal variability (Screen *et al* 2013, McCusker *et al* 2016, Sun *et al* 2016). In this context, the changes in the $WACE_{Mean}$ may primarily result from internal variability within the extratropical atmosphere (Sun *et al* 2016, Jin *et al* 2020, Wang and Chen 2022). Regardless of whether the change in $WACE_{Mean}$ is driven by sea ice loss, the upper-level Ural blocking highs and the surface Siberian highs are important factors influencing the variability of the $WACE_{Mean}$ (Mori *et al* 2014). These circulation features are also dominant factors associated with cold extremes in Eurasia, particularly in East Asia (Zhang *et al* 1997, Wang *et al* 2010, Park *et al* 2011, Cheung *et al* 2012). Hence, changes in the phase of the $WACE_{Mean}$ potentially have implications for modulating Eurasian cold extremes.

Previous research has delved into the impact of the $WACE_{Mean}$ on the winter-mean climate anomalies and the frequency of cold extremes in the Eurasia region (Mori *et al* 2014, 2019, Wang *et al* 2020a). Notably, the variation in the WACE pattern has been observed on subseasonal timescale in addition to the seasonal timescale (Yao *et al* 2017, Kim *et al* 2021). This highlights the necessity to investigate the influence of the subseasonal variability of the WACE pattern ($WACE_{SSV}$), as changes at this timescale can have significant implications for society and ecosystems, particularly if they lead to altered extreme events (Katz and Brown 1992, Schär *et al* 2004, Martineau *et al* 2020, van der Wiel and Bintanja 2021). Consequently, this research also aims to examine whether changes in the $WACE_{SSV}$ can modify the relationship between the $WACE_{Mean}$ and the frequency of cold extremes in Eurasia. By doing so, valuable insights can be gained into the complex mechanisms by which the WACE pattern influences cold extremes in Eurasia.

2. Data and methods

This study primarily utilizes daily and monthly reanalysis data from the European Centre for Medium-Range Weather Forecasts reanalysis version 5 (ERA5) dataset (Hersbach *et al* 2020). The daily and monthly-mean variables are derived from hourly data and include surface air temperature (SAT), sea level pressure (SLP) and 500 hPa geopotential height (Z500). The selected temporal and spatial ranges are from January 1950 to March 2023, with a resolution of $1^\circ \times 1^\circ$. In a study conducted by Yu *et al* (2021), it was found that the ERA5 temperature field shows good consistency with buoy observations, although there may be some warm biases present. This confirms the reliability of ERA5 data in accurately reflecting climate variations in the Arctic region.

The calculation of daily anomalies for any variable was conducted using the following procedure: firstly, a 10 d low-pass filter was applied to the daily mean atmospheric data in order to eliminate fluctuations associated with synoptic-scale baroclinic waves. Subsequently, for a specific date, an anomaly field was defined as the deviation of the low-pass filtered field for that particular date from the daily climatological-mean annual cycle. In order to quantify the strength of subseasonal variability (SSV), the standard deviation of the daily anomalies was calculated for each grid point during the winter season (December–February, DJF) for each year. This methodology aligned with the approach presented in Nakamura (1996). To identify cold extreme dates, the daily SAT anomalies were compared to the 5th percentile of the distribution of SAT anomalies for the winter season spanning from 1950/51 to 2022/23. Cold extreme dates were determined as instances when the SAT anomaly fell below this threshold, using the methodology employed in Martineau *et al* (2020). Blocking events in this study were defined following the method used in previous studies (Liu *et al* 2012, Tang *et al* 2013). Specifically, blocking events were identified as intervals when the daily SLP anomalies were higher than 1.5 standard deviations from the climatological mean for each grid cell, persisting for a minimum duration of five consecutive days.

To extract the WACE pattern, an empirical orthogonal function (EOF) analysis was employed, as done in previous studies (Mori *et al* 2014, Wang *et al* 2020a). In this study, the EOF analysis was applied to the daily SAT anomalies during winter, covering the region from 0° to 180° E and 30° to 90° N, over the period from 1950/51 to 2022/23. To ensure equal weighting of areas in the analysis, the SAT anomalies were weighted by the cosine of latitude, providing equal weightage to individual grid points (North *et al* 1982). The two leading EOF patterns explained approximately 33% of the total variance. The first leading EOF pattern (EOF1) accounted for 20% of the total variance and showed SAT anomalies associated with the Arctic oscillation (AO) (figure S1(a)). The second leading EOF pattern (EOF2) accounted for 13% of the total variance and exhibited the typical WACE anomaly pattern, featuring pronounced warming over the Barents-Kara region and significant cooling spreading over the central and eastern parts of the Eurasian continent (figure S1(b)). Therefore, the second principal component (PC2) was considered as the WACE index. Subsequently, the winter-mean state and SSV of the WACE pattern were quantified as the $WACE_{Mean}$ index and $WACE_{SSV}$ index, respectively. The $WACE_{Mean}$ index represents the average value of daily WACE index during the winter season of each year. On the other hand, the $WACE_{SSV}$ index is calculated as the standard deviation of the daily WACE index during the winter season for each year.

3. Results

3.1. Influence of $WACE_{Mean}$ and $WACE_{SSV}$ on Eurasian cold extremes

To investigate the climatic influence of the $WACE_{Mean}$ and $WACE_{SSV}$, we analyze the regressed anomalies of winter-mean SAT (SAT_{Mean}), SSV of SAT (SAT_{SSV}), and cold extreme frequency onto the normalized $WACE_{Mean}$ index and $WACE_{SSV}$ index, respectively. As depicted in figures 1(a) and (d), the regressed patterns of SAT_{Mean} on the normalized $WACE_{Mean}$ index and $WACE_{SSV}$ index exhibit distinct differences. Additionally, the associated anomalous patterns of SAT_{SSV} with the two indices are also markedly different (figures 1(b) and (e)). However, the positive values of both indices demonstrate an increasing tendency in the frequency of cold extremes over central Eurasia and East Asia (figures 1(c) and (f)). These changes in cold extreme frequency, which are associated with the $WACE_{Mean}$, are primarily driven by the variations in SAT_{Mean}. When the $WACE_{Mean}$ is in its positive phase, cold extremes occur more frequently in regions of central Eurasia and East Asia where SAT_{Mean} is colder, while they are less frequent in the Barents–Kara Sea regions where SAT_{Mean} is warmer (figures 1(a) and (c)). In contrast, the regressed pattern of SAT_{SSV} onto the normalized $WACE_{Mean}$ index is very different from the regressed pattern of cold extreme frequency (figures 1(b) and (c)). This suggests a limited influence of associated anomalous SAT_{SSV} on the frequency of extreme cold events.

On the other hand, a stronger $WACE_{SSV}$ corresponds to a significant enhancement in SAT_{SSV} but no significant changes in the SAT_{Mean} in central Eurasia and East Asia (figures 1(d) and (e)). A study conducted by Song et al (2018) has emphasized the crucial role of subseasonal variations in triggering cold events in East Asia, with more than half of the temperature anomalies attributed to these variations. In this context, a stronger SAT_{SSV}, which corresponds to a wider range of subseasonal SAT fluctuations, can also increase the likelihood of cold extremes. Therefore, even in the absence of significant reductions in SAT_{Mean}, the enhanced SAT_{SSV} in central Eurasia and East Asia, associated with a stronger $WACE_{SSV}$, also contributes to an increased likelihood of cold extreme in these regions (figures 1(d)–(f)). Furthermore, it is observed that a stronger $WACE_{SSV}$ corresponds to enhanced SAT_{SSV} over the Barents-Kara Sea region, but it does not have a significant impact on the frequency of cold extremes in this particular region (figures 1(e) and (f)). This can likely be attributed to the primary influence of other factors, such as $WACE_{Mean}$, in determining extreme cold events in the Arctic region, as depicted in figures 1(a) and (c). Furthermore, although a stronger $WACE_{SSV}$ corresponds to a decrease in SAT_{Mean} anomalies over high-latitude regions of the Eurasian continent, these SAT_{Mean} anomalies do not translate into changes in the frequency of cold extremes (figures 1(d) and (f)).

As previous studies have indicated, variations in SAT on both subseasonal and seasonal timescales over the Eurasian continent are closely linked to changes in atmospheric circulation anomalies (Wang and Chen 2014, Song and Wu 2017). Therefore, further investigation was conducted into the changes in the anomalies of winter-mean atmospheric circulation and the strength of the subseasonal circulation fluctuations, represented by the SSV of SLP (SLP_{SSV}) and Z500 ($Z500_{SSV}$). Figure 2 displays the regressed anomalies of winter-mean SLP (SLP_{Mean}), SLP_{SSV} and blocking frequency onto the standardized time series of $WACE_{Mean}$ index and $WACE_{SSV}$ index, respectively. We observe that the positive phase of $WACE_{Mean}$ is associated with positive anomalies in SLP_{Mean} over the Ural–Siberian region (figure 2(a)). This indicates a strengthening of the surface Siberian High, which is a direct dynamical factor to link warm Arctic to cold Eurasia (Wu et al 2015, Wu 2017, Wu and Ding 2023). Meanwhile, there are significant increases in winter-mean Z500 ($Z500_{Mean}$) around the Ural Mountains during the positive phase of $WACE_{Mean}$ (figure S3(a)). These findings are consistent with previous research conducted by Mori et al (2014). Additionally, we observed that the strength of the subseasonal circulation fluctuations over the Ural region, represented by the SLP_{SSV} and $Z500_{SSV}$, tends to be more pronounced during the positive phase of $WACE_{Mean}$ (figures 2(b) and S3(b)). The amplification of subseasonal circulation fluctuations may be attributed to the fact that the positive phase of $WACE_{Mean}$ corresponds to reduced temperature gradients (figure 1(a)) and a more meandering jet, which are favorable for the development of subseasonal Rossby waves (Francis and Vavrus 2012, Liu et al 2012, Tang et al 2013). The presence of positive winter-mean anticyclonic anomalies, coupled with a wider range of subseasonal fluctuations in atmospheric circulation, results in an increased probability

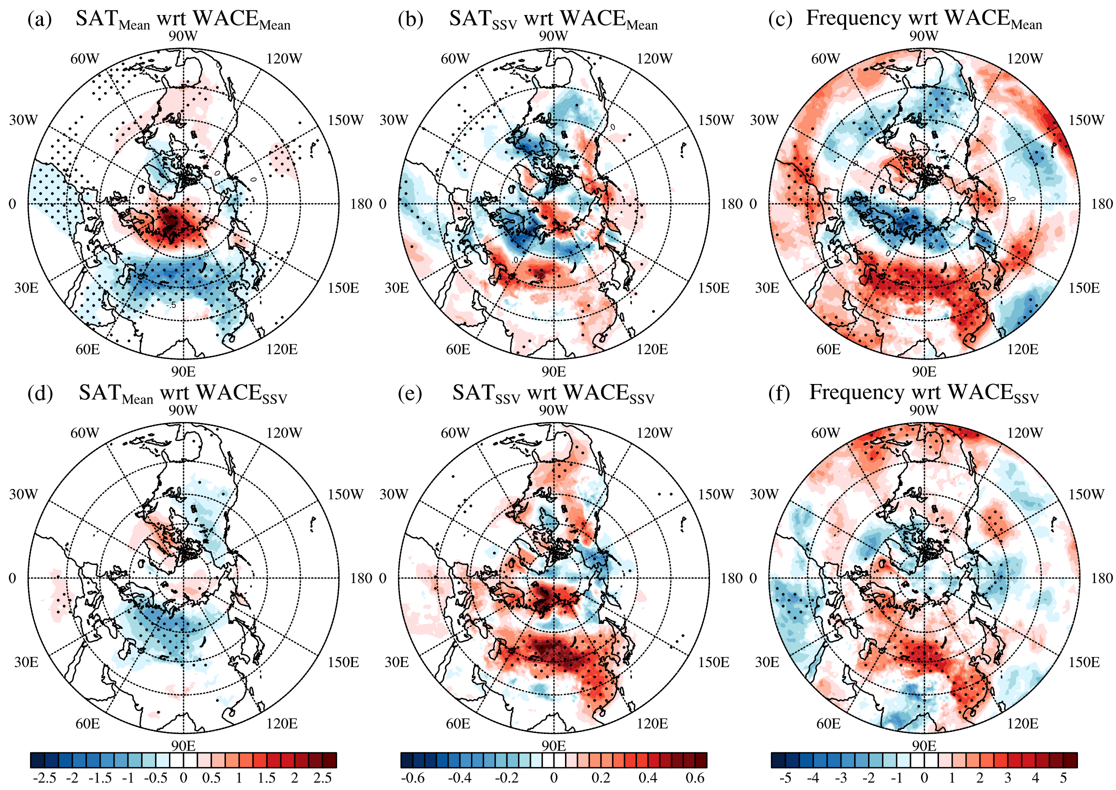

Figure 1. Regressed anomalies of (a) SAT_{Mean} (°C), (b) SAT_{SSV} (°C) and (c) cold extreme frequency (%) onto the standardized time series of $WACE_{Mean}$ index. (d)–(f) are the same as (a)–(c), but for the regressed anomalies onto the standardized time series of $WACE_{SSV}$ index. The dotted areas denote the anomalies that are significant at the 95% confidence level according to the Student's t-test.

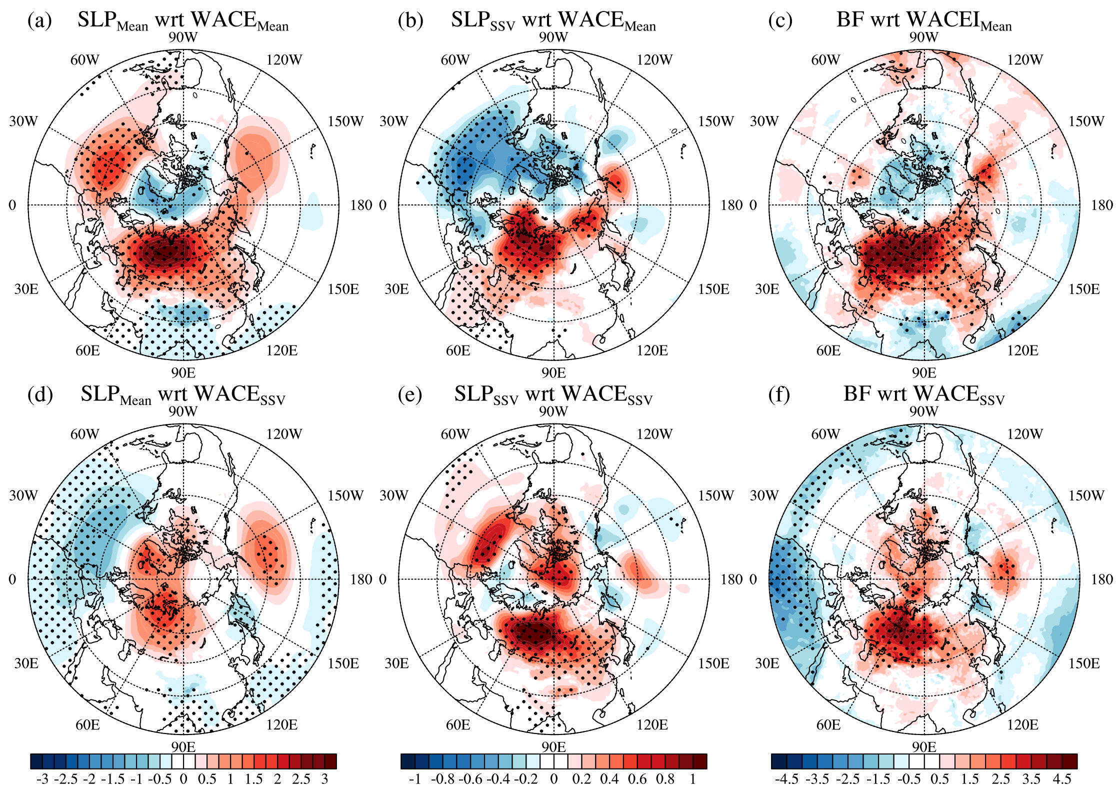

Figure 2. Regressed anomalies of (a) SLP_{Mean} (hPa), (b) SLP_{SSV} (hPa) and (c) blocking frequency (%) onto the standardized time series of $WACE_{Mean}$ index. (d)–(f) are the same as (a)–(c), but for the regressed anomalies onto the standardized time series of $WACE_{SSV}$ index. The dotted areas denote the anomalies that are significant at the 95% confidence level according to the Student's t-test.

of blocking events occurring over the Ural–Siberian region (figure 2(c)).

The positive $WACE_{SSV}$ index is associated with positive SLP_{Mean} anomalies over the Ural region and increased SLP_{SSV} anomalies over the Ural–Siberian region (figures 2(d) and (e)). These anomalies also contribute to an increased likelihood of blocking events occurring over the Ural–Siberian region (figure 2(f)). The variations in the $WACE_{SSV}$ are highly correlated with changes in both SLP_{SSV} and $Z500_{SSV}$ (figures 2(e) and S3(d)). However, in the corresponding winter-mean anomalies, only significant changes are observed in SLP_{Mean} and not in $Z500_{Mean}$ (figures 2(d) and S3(b)). The SLP_{Mean} anomalies associated with a stronger $WACE_{SSV}$ display characteristics similar to the negative phase of AO (figure 2(d)). This finding is consistent with previous research indicating that the negative winter-mean AO is associated with an enhancement in subseasonal temperature variability in Eurasia (Gong and Ho 2004, Jeong and Ho 2005).

In summary, the SLP_{Mean} and SLP_{SSV} anomalies associated with both $WACE_{Mean}$ and $WACE_{SSV}$ contribute to altering the likelihood of events over the Ural–Siberian region. Since blocking events in this region play a vital role in the occurrence of cold extremes across central Eurasia and East Asia (Yao *et al* 2017, Ma *et al* 2018), the probability of experiencing cold extremes in these regions undergoes significant changes associated with variations in both $WACE_{Mean}$ index and $WACE_{SSV}$ index.

3.2. Modulation of the influence of $WACE_{Mean}$ on Eurasian cold extremes by $WACE_{SSV}$

The aforementioned findings suggest that both of the $WACE_{Mean}$ and $WACE_{SSV}$ can significantly impact extreme cold events in central Eurasia and East Asia. Importantly, since the interannual variations of these two factors are independent, with a correlation coefficient of only 0.14 between the detrended time series of the two indices, their effects on the Eurasian cold extremes can be either consistent or contrasting. To investigate whether the $WACE_{SSV}$ can modulate the influence of the $WACE_{Mean}$ on Eurasian cold extremes, the years with a positive $WACE_{Mean}$ index were divided into two groups: $+WACE_{Mean}/+WACE_{SSV}$ years when the normalized $WACE_{SSV}$ index is larger than zero, and $+WACE_{Mean}/-WACE_{SSV}$ years when the $WACE_{SSV}$ index is less than zero. This resulted in 18 yr identified as $+WACE_{Mean}/+WACE_{SSV}$ years and 19 yr as $+WACE_{Mean}/-WACE_{SSV}$ years. Figures 3(a) and (b) examines the composite frequency anomalies of cold extremes during $+WACE_{Mean}/+WACE_{SSV}$ years and $+WACE_{Mean}/-WACE_{SSV}$ years. The composite anomalies during $+WACE_{Mean}/+WACE_{SSV}$ years exhibit a well-organized and statistically significant pattern. Notably, a significant increase in the frequency of cold extremes can be observed over central Eurasia and East Asia during $+WACE_{Mean}/+WACE_{SSV}$ years (figure 3(a)). In contrast, during $+WACE_{Mean}/-WACE_{SSV}$ years, the anomalies of the cold extreme frequency nearly disappear over the Eurasian continent (figure 3(b)). This finding suggests that, when the $WACE_{SSV}$ index is negative, the positive phase of the $WACE_{Mean}$ no longer promotes the occurrence of cold extremes over Eurasia. Therefore, it can be concluded that the $WACE_{SSV}$ greatly modulates the influence of the $WACE_{Mean}$ on Eurasian cold extremes.

In consideration of the crucial role played by blocking events over the Ural-Siberian region in driving Eurasian cold extremes, we further examined the composite anomalies of blocking frequency during the $+WACE_{Mean}/+WACE_{SSV}$ years and $+WACE_{Mean}/-WACE_{SSV}$ years. As depicted in figures 3(c) and (d), the differences in the distribution of cold extreme frequency anomalies between the two sets of years can be attributed to variations in the frequency of blocking events over the Ural–Siberian region. Figure 3(c) shows a significant increase in blocking frequency over the Ural–Siberian region during $+WACE_{Mean}/+WACE_{SSV}$ years, corresponding to the heightened occurrence of cold extremes observed across central Eurasia and East Asia. Conversely, figure 3(d) shows no significant change in Ural–Siberian blocking frequency during $+WACE_{Mean}/-WACE_{SSV}$ years, resulting in no significant anomalies in the frequency of cold extremes in Eurasia. These results suggest that the modulation by the $WACE_{SSV}$ influences the frequency of blocking events over the Ural–Siberian region. This modulation, in turn, affects the occurrence frequency of cold extremes in central Eurasia and East Asia.

One question that arises is the possible mechanism responsible for the difference in blocking frequency anomalies between the $+WACE_{Mean}/+WACE_{SSV}$ and $+WACE_{Mean}/-WACE_{SSV}$ years. To understand this, we examine the composite patterns of SLP_{Mean} and SLP_{SSV} anomalies for the $+WACE_{Mean}/+WACE_{SSV}$ and $+WACE_{Mean}/-WACE_{SSV}$ years in figure 4, considering their crucial role in altering blocking frequency. In figures 4(a) and (b), both the $+WACE_{Mean}/+WACE_{SSV}$ and $+WACE_{Mean}/-WACE_{SSV}$ years exhibit pronounced increases in SLP_{Mean} anomalies in the northern part of the Eurasian continent. These anomalies closely resemble the regression pattern associated with the positive $WACE_{Mean}$ shown in figure 2(a). This suggests that the constructive and destructive superposition of the SLP_{Mean} anomalies related to the $WACE_{Mean}$ and $WACE_{SSV}$ plays a limited role in explaining the differences in blocking frequency anomalies. However, there are substantial differences in the composite patterns of SLP_{SSV} anomalies between the two groups. In $+WACE_{Mean}/+WACE_{SSV}$ years, the constructive superposition of SLP_{SSV}

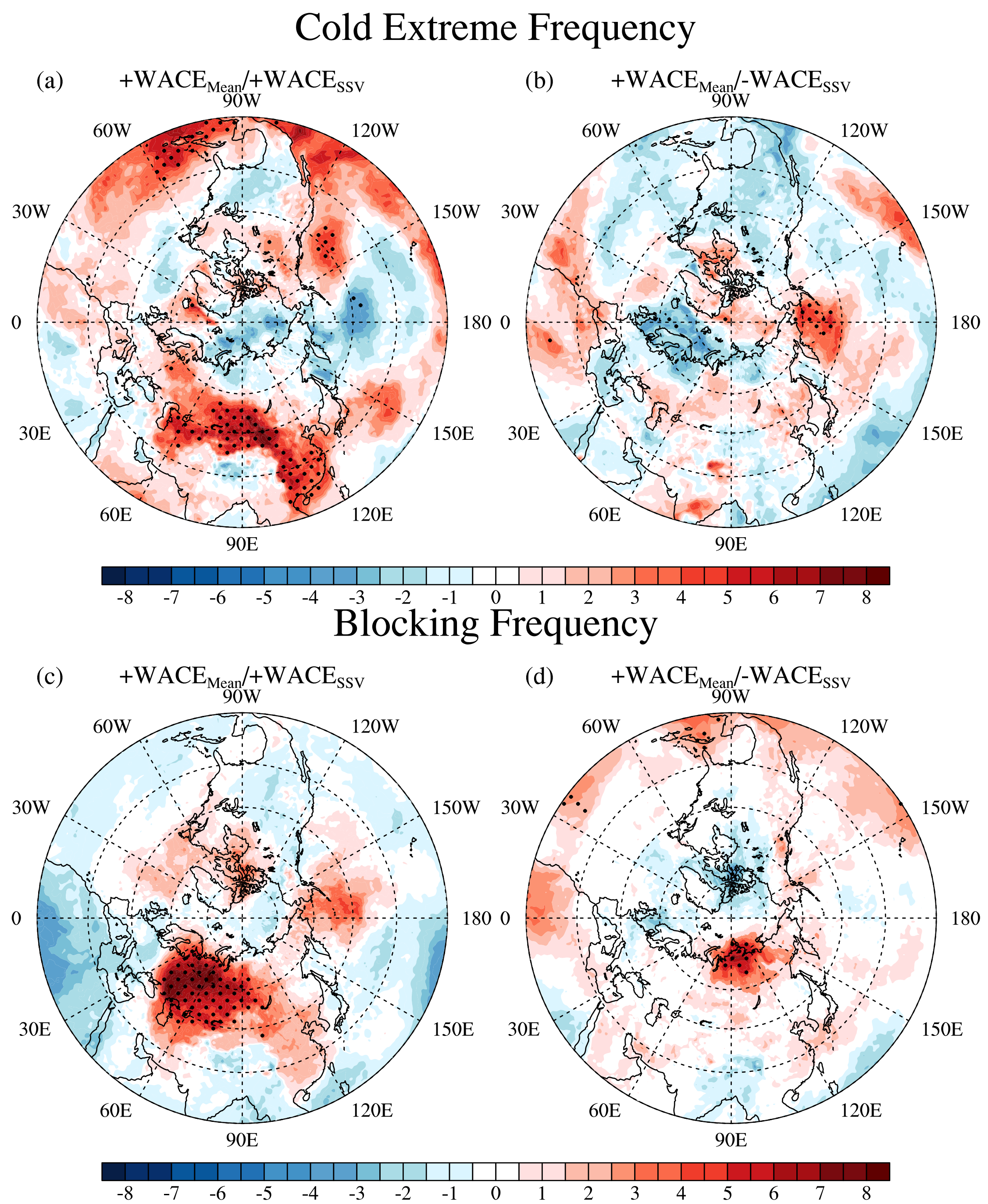

Figure 3. Composite anomalies of cold extreme frequency (%) for (a) +WACE$_{Mean}$/+WACE$_{SSV}$ and (b) +WACE$_{Mean}$/−WACE$_{SSV}$ years, respectively. (c), (d) are the same as (a), (b), but for the blocking frequency (%) anomalies. The dotted areas denote the anomalies that are significant at the 95% confidence level according to the Student's t-test.

anomalies related to the WACE$_{Mean}$ and WACE$_{SSV}$ leads to a significant enhancement of SLP$_{SSV}$ over the Ural–Siberia region. This enhancement aligns closely with the regions of positive SLP$_{Mean}$ anomalies (figures 4(a) and (c)). Consequently, the combined effect results in an increase in the frequency of blocking events in the region. In contrast, during +WACE$_{Mean}$/−WACE$_{SSV}$ years, the destructive superposition of SLP$_{SSV}$ anomalies leads to no significant changes in SLP$_{SSV}$ over the northern Eurasian continent (figure 4(d)). Without a notable enhancement in subseasonal SLP fluctuations, the increase in SLP$_{Mean}$ alone does not seem sufficient to influence the blocking frequency over the northern Eurasian region. These findings indicate that the differences in the distribution of blocking frequency anomalies in the Ural-Siberian region can be partly attributed to the constructive and destructive superposition of SLP$_{SSV}$ anomalies related to the WACE$_{Mean}$ and WACE$_{SSV}$.

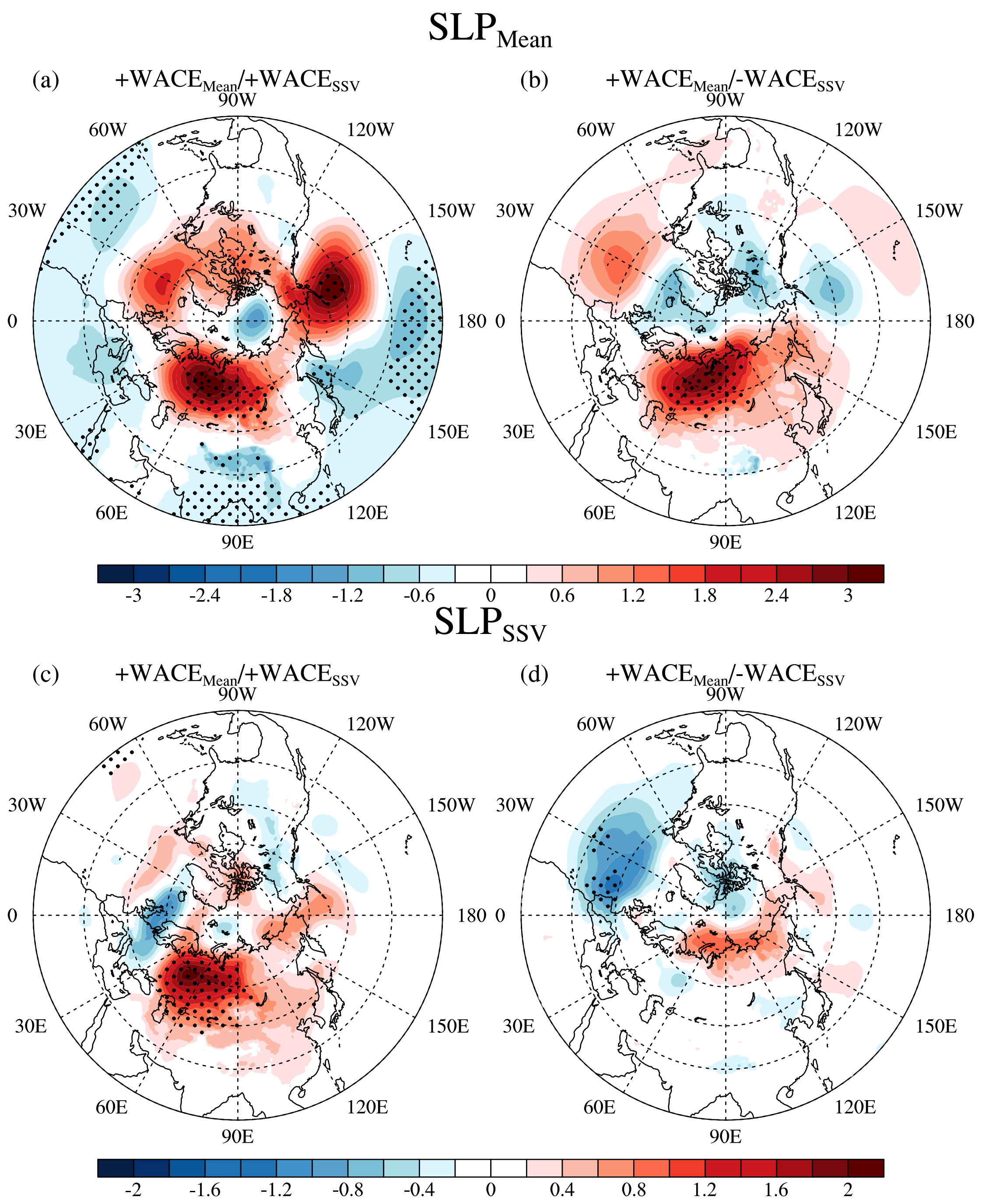

Figure 4. Composite anomalies of SLP_{Mean} (hPa) for (a) $+WACE_{Mean}/+WACE_{SSV}$ and (b) $+WACE_{Mean}/-WACE_{SSV}$ years, respectively. (c), (d) are the same as (a), (b), but for the SLP_{SSV} (hPa). The dotted areas denote the anomalies that are significant at the 95% confidence level according to the Student's t-test.

4. Summary and discussion

Utilizing ERA5 data, this study has found that both the $WACE_{Mean}$ and $WACE_{SSV}$ play significant roles in shaping cold extremes over Eurasia. The frequency of cold extremes in Eurasia shows an increasing tendency associated with the positive $WACE_{Mean}$, primarily driven by variations in SAT_{Mean}. Regions with colder SAT_{Mean}, such as central Eurasia and East Asia, exhibit more frequent cold extremes. Additionally, a stronger $WACE_{SSV}$ corresponds to an enhancement of SAT_{SSV} in Eurasia, particularly in central Eurasia and East Asia. This wider range of subseasonal SAT fluctuations also contributes to an increased likelihood of extreme events in these regions.

The study further reveals that the $WACE_{SSV}$ modulates the influence of the $WACE_{Mean}$ on Eurasian cold extremes. Specifically, during years with both a positive $WACE_{Mean}$ and enhanced $WACE_{SSV}$ ($+WACE_{Mean}/+WACE_{SSV}$ years), there is a notable increase in the occurrence of cold extremes over central Eurasia and East Asia. Conversely, during years with a positive $WACE_{Mean}$ but reduced $WACE_{SSV}$ ($+WACE_{Mean}/-WACE_{SSV}$ years), the anomalies in cold extreme frequency diminish. These differences can be attributed to changes in blocking frequency over the Ural-Siberian region. The $+\mathrm{WACE_{Mean}}/+\mathrm{WACE_{SSV}}$ years exhibit a significant increase in blocking frequency, corresponding to the heightened occurrence of cold extremes in central Eurasia and East Asia. However, the $+\mathrm{WACE_{Mean}}/-\mathrm{WACE_{SSV}}$ years show no significant changes in blocking frequency, leading to no significant anomalies in cold extreme frequency in this region.

An analysis of the underlying mechanisms reveals that the constructive and destructive superposition of $\mathrm{SLP_{SSV}}$ associated with the $\mathrm{WACE_{Mean}}$ and $\mathrm{WACE_{SSV}}$ play a crucial role in shaping the blocking frequency over Ural–Siberian region. During $+\mathrm{WACE_{Mean}}/+\mathrm{WACE_{SSV}}$ years, due to the constructive superposition of $\mathrm{SLP_{SSV}}$ anomalies related to the $\mathrm{WACE_{Mean}}$ and $\mathrm{WACE_{SSV}}$, there is an enhancement of subseasonal SLP fluctuations over the Ural-Siberia region, closely aligned with the regions of positive winter-mean SLP anomalies. This combined effect leads to an increase in blocking activity and the occurrence of cold extremes. Conversely, during $+\mathrm{WACE_{Mean}}/-\mathrm{WACE_{SSV}}$ years, the destructive superposition of the $\mathrm{SLP_{SSV}}$ anomalies associated with $\mathrm{WACE_{Mean}}$ and $\mathrm{WACE_{SSV}}$ results in no significant changes in subseasonal SLP fluctuations over the northern Eurasian continent. In the absence of a substantial enhancement in subseasonal SLP fluctuations, the increase in $\mathrm{SLP_{Mean}}$ is not sufficient to significantly alter the blocking frequency over the northern Eurasian region.

In this study, blocking events were defined as positive SLP anomalies that persist for an extended period. Previous studies have commonly used the two-dimensional blocking index, calculated using meridional gradients of Z500, to detect blocking events (Davini *et al* 2012, Wang *et al* 2021). Applying this method, we also observed a significant increase in the frequency of blocking events around the Ural Mountains during the positive phase of the $\mathrm{WACE_{Mean}}$ or with a stronger $\mathrm{WACE_{SSV}}$. However, it is important to note that the positive anomalies in blocking frequency, determined by meridional gradients of Z500, are primarily observed in the Ural region and do not extend to the Siberian region (figure S4). Furthermore, the modulation of the influence of the $\mathrm{WACE_{Mean}}$ on blocking events by the $\mathrm{WACE_{SSV}}$ remains evident even when using the method of meridional height gradients (figure S5), enhancing the reliability and robustness of our conclusions.

Our study highlights the importance of understanding the mechanisms driving changes in $\mathrm{WACE_{SSV}}$. Previous studies have indicated a decrease in $\mathrm{SAT_{SSV}}$ over northern high latitudes during winter due to the decreased meridional temperature gradients associated with Arctic amplification (Screen 2014, Collow *et al* 2019, Blackport *et al* 2021, Dai and Deng 2021). Blackport *et al* (2021) further suggested that the decreasing $\mathrm{SAT_{SSV}}$ in the northern extratropics is attributed to human influence. However, it is worth noting that the weakening in $\mathrm{SAT_{SSV}}$ primarily occurs in high-latitude regions and not in central Eurasia and East Asia, indicating limited impact from anthropogenic forcing on $\mathrm{WACE_{SSV}}$. Previous studies have emphasized the influence of the winter-mean AO on $\mathrm{SAT_{SSV}}$ in East Asia, based on observed statistical connections (Gong and Ho 2004, Jeong and Ho 2005). This highlights the potential impact of the atmospheric mean flow on $\mathrm{WACE_{SSV}}$, given the close linkage between $\mathrm{WACE_{SSV}}$ and $\mathrm{SAT_{SSV}}$ in East Asia. However, it is important to note that the change in $\mathrm{WACE_{SSV}}$ cannot be simply attributed to the anomalous atmospheric mean flow. This is because changes in the self-interaction among associated subseasonal eddies can also alter the seasonal-mean flow (Cai and Van Den Dool 1994, Feldstein 2002, 2003). Therefore, further investigation is necessary to better understand the relationship between the winter-mean flow and $\mathrm{WACE_{SSV}}$.

Data availability statement

The hourly ERA5 data are available through the Copernicus Climate Data Store (https://cds.climate.copernicus.eu/cdsapp#!/dataset/reanalysis-era5-single-levels?tab=form and https://cds.climate.copernicus.eu/cdsapp#!/dataset/reanalysis-era5-pressure-levels?tab=form).

No new data were created or analysed in this study.

Acknowledgments

We thank three anonymous reviewers for their constructive suggestions, which helped to improve the paper. This work was supported by the National Natural Science Foundation of China (42122047, 42206208 and 42105036) and the Basic Research Fund of CAMS (2021Y021, 2021Z006, 2023Z015, 2023Z004 and 2023Z025).

Conflict of interest

The authors declare that they have no conflict of interest.

ORCID iDs

Sai Wang https://orcid.org/0000-0002-4648-0439
Wen Chen https://orcid.org/0000-0001-9327-9079

References

Alexander L V *et al* 2006 Global observed changes in daily climate extremes of temperature and precipitation *J. Geophys. Res. Atmos.* **111** D05109

Blackport R, Fyfe J C and Screen J A 2021 Decreasing subseasonal temperature variability in the northern extratropics attributed to human influence *Nat. Geosci.* **14** 719–23
Blackport R and Screen J A 2020 Weakened evidence for mid-latitude impacts of Arctic warming *Nat. Clim. Chang.* **10** 1065–6
Blackport R and Screen J A 2021 Observed statistical connections overestimate the causal effects of Arctic Sea ice changes on midlatitude winter climate *J. Clim.* **34** 3021–38
Cai M and Van Den Dool H M 1994 Dynamical decomposition of low-frequency tendencies *J. Atmos. Sci.* **51** 2086–100
Cheung H Nam, Zhou W, Mok H Yim and Wu M Chi 2012 Relationship between Ural–Siberian blocking and the East Asian Winter monsoon in relation to the Arctic Oscillation and the El Niño–Southern Oscillation *J. Clim.* **25** 4242–57
Cohen J L, Furtado J C, Barlow M A, Alexeev V A and Cherry J E 2012 Arctic warming, increasing snow cover and widespread boreal winter cooling *Environ. Res. Lett.* **7** 014007
Cohen J *et al* 2020 Divergent consensuses on Arctic amplification influence on midlatitude severe winter weather Nat. Clim. Chang. **10** 20–29
Cohen J, Screen J A, Furtado J C, Barlow M, Whittleston D, Coumou D, Francis J, Dethloff K, Entekhabi D and Overland J 2014 Recent Arctic amplification and extreme mid-latitude weather *Nat. Geosci.* **7** 627–37
Collow T W, Wang W and Kumar A 2019 Reduction in Northern midlatitude 2-m temperature variability due to Arctic Sea Ice loss *J. Clim.* **32** 5021–35
Dai A and Deng J 2021 Arctic amplification weakens the variability of daily temperatures over northern middle-high latitudes *J. Clim.* **34** 2591–609
Davini P, Cagnazzo C, Gualdi S and Navarra A 2012 Bidimensional diagnostics, variability, and trends of northern hemisphere blocking *J. Clim.* **25** 6496–509
Feldstein S B 2002 Fundamental mechanisms of the growth and decay of the PNA teleconnection pattern *Q. J. R. Meteorol. Soc.* **128** 775–96
Feldstein S B 2003 The dynamics of NAO teleconnection pattern growth and decay *Q. J. R. Meteorol. Soc.* **129** 901–24
Francis J A and Vavrus S J 2012 Evidence linking Arctic amplification to extreme weather in mid-latitudes *Geophys. Res. Lett.* **39** L06801
Gong D-Y and Ho C-H 2004 Intra-seasonal variability of wintertime temperature over East Asia *Int. J. Climatol.* **24** 131–44
Gong Z, Feng G, Ren F and Li J 2014 A regional extreme low temperature event and its main atmospheric contributing factors *Theor. Appl. Climatol.* **117** 195–206
Herring S C, Hoell A, Hoerling M P, Kossin J P, Schreck C J and Stott P A 2016 Explaining extreme events of 2015 from a climate perspective *Bull. Am. Meteorol. Soc.* **97** S1–S145
Hersbach H *et al* 2020 The ERA5 global reanalysis *Q. J. R. Meteorol. Soc.* **146** 1999–2049
Honda M, Inoue J and Yamane S 2009 Influence of low Arctic sea-ice minima on anomalously cold Eurasian winters *Geophys. Res. Lett.* **36** L08707
Jeong J-H and Ho C-H 2005 Changes in occurrence of cold surges over east Asia in association with Arctic oscillation *Geophys. Res. Lett.* **32** L14704
Jin C, Wang B, Yang Y-M and Liu J 2020 Warm Arctic-Cold Siberia" as an internal mode instigated by North Atlantic warming *Geophys. Res. Lett.* **47** e2019GL086248
Johnson N C, Xie S-P, Kosaka Y and Li X 2018 Increasing occurrence of cold and warm extremes during the recent global warming slowdown *Nat. Commun.* **9** 1724
Katz R W and Brown B G 1992 Extreme events in a changing climate: variability is more important than averages *Clim. Change* **21** 289–302
Kim H-J, Son S-W, Moon W, Kug J-S and Hwang J 2021 Subseasonal relationship between Arctic and Eurasian surface air temperature *Sci. Rep.* **11** 4081
Koenigk T *et al* 2019 Impact of Arctic sea ice variations on winter temperature anomalies in northern hemispheric land areas *Clim. Dyn.* **52** 3111–37
Komatsu K K, Takaya Y, Toyoda T and Hasumi H 2022 Response of Eurasian temperature to Barents–Kara Sea ice: evaluation by multi-model seasonal predictions *Geophys. Res. Lett.* **49** e2021GL097203
Liu J, Curry J A, Wang H, Song M and Horton R M 2012 Impact of declining Arctic sea ice on winter snowfall *Proc. Natl Acad. Sci.* **109** 4074–9
Ma S, Zhu C, Liu B, Zhou T, Ding Y and Orsolini Y J 2018 Polarized response of East Asian winter temperature extremes in the era of Arctic warming *J. Clim.* **31** 5543–57
Martineau P, Nakamura H, Kosaka Y, Taguchi B and Mori M 2020 Modulations of North American and European weather variability and extremes by interdecadal variability of the atmospheric circulation over the North Atlantic sector *J. Clim.* **33** 8125–46
McCusker K E, Fyfe J C and Sigmond M 2016 Twenty-five winters of unexpected Eurasian cooling unlikely due to Arctic sea-ice loss *Nat. Geosci.* **9** 838–42
Mori M, Kosaka Y, Watanabe M, Nakamura H and Kimoto M 2019 A reconciled estimate of the influence of Arctic sea-ice loss on recent Eurasian cooling *Nat. Clim. Change* **9** 123–9
Mori M, Watanabe M, Shiogama H, Inoue J and Kimoto M 2014 Robust Arctic sea-ice influence on the frequent Eurasian cold winters in past decades *Nat. Geosci.* **7** 869–73
Nakamura H 1996 Year-to-Year and interdecadal variability in the activity of intraseasonal fluctuations in the Northern Hemisphere wintertime circulation *Theor. Appl. Climatol.* **55** 19–32
North G R, Moeng F J, Bell T L and Cahalan R F 1982 The latitude dependence of the variance of zonally averaged quantities *Mon. Weather Rev.* **110** 319–26
Ogawa F *et al* 2018 Evaluating impacts of recent Arctic Sea ice loss on the Northern hemisphere winter climate change *Geophys. Res. Lett.* **45** 3255–63
Outten S *et al* 2023 Reconciling conflicting evidence for the cause of the observed early 21st century Eurasian cooling *Weather Clim. Dyn.* **4** 95–114
Overland J E, Wood K R and Wang M 2011 Warm Arctic-cold continents: climate impacts of the newly open Arctic Sea *Polar Res.* **30** 15787
Park T, Ho C and Yang S 2011 Relationship between the Arctic Oscillation and Cold Surges over East Asia *J. Clim.* **24** 68–83
Peterson T C, Stott P A and Herring S 2012 Explaining extreme events of 2011 from a climate perspective *Bull. Am. Meteorol. Soc.* **93** 1041–67
Schär C, Vidale P L, Lüthi D, Frei C, Häberli C, Liniger M A and Appenzeller C 2004 The role of increasing temperature variability in European summer heatwaves *Nature* **427** 332–6
Schoetter R, Cattiaux J and Douville H 2015 Changes of western European heat wave characteristics projected by the CMIP5 ensemble *Clim. Dyn.* **45** 1601–16
Screen J A 2014 Arctic amplification decreases temperature variance in northern mid- to high-latitudes *Nat. Clim. Change* **4** 577–82
Screen J A, Deser C and Sun L 2015 Reduced risk of North American cold extremes due to continued Arctic Sea ice loss *Bull. Am. Meteorol. Soc.* **96** 1489–503
Screen J A, Simmonds I, Deser C and Tomas R 2013 The atmospheric response to three decades of observed Arctic Sea ice loss *J. Clim.* **26** 1230–48
Song L and Wu R 2017 Processes for occurrence of strong cold events over Eastern China *J. Clim.* **30** 9247–66
Song L, Wu R and Jiao Y 2018 Relative contributions of synoptic and intraseasonal variations to strong cold events over eastern China *Clim. Dyn.* **50** 4619–34
Stott P A, Stone D A and Allen M R 2004 Human contribution to the European heatwave of 2003 *Nature* **432** 610–4

Sun L, Perlwitz J and Hoerling M 2016 What caused the recent "Warm Arctic, Cold Continents" trend pattern in winter temperatures? *Geophys. Res. Lett.* **43** 5345–52
Tang Q, Zhang X, Yang X and Francis J A 2013 Cold winter extremes in northern continents linked to Arctic sea ice loss *Environ. Res. Lett.* **8** 014036
van der Wiel K and Bintanja R 2021 Contribution of climatic changes in mean and variability to monthly temperature and precipitation extremes *Commun. Earth Environ.* **2** 1
Wang L and Chen W 2014 The East Asian winter monsoon: re-amplification in the mid-2000s *Chin. Sci. Bull.* **59** 430–6
Wang L, Chen W, Zhou W, Chan J C, Barriopedro D and Huang R 2010 Effect of the climate shift around mid 1970s on the relationship between wintertime Ural blocking circulation and East Asian climate *Int. J. Climatol.* **30** 153–8
Wang S and Chen W 2022 Impact of internal variability on recent opposite trends in wintertime temperature over the Barents–Kara Seas and central Eurasia *Clim. Dyn.* **58** 2941–56
Wang S, Nath D and Chen W 2021 Nonstationary relationship between sea ice over Kara–Laptev seas during August–September and Ural blocking in the following winter *Int. J. Climatol.* **41** E1608–E22
Wang S, Nath D, Chen W and Ma T 2020a CMIP5 model simulations of warm Arctic-cold Eurasia pattern in winter surface air temperature anomalies *Clim. Dyn.* **54** 4499–513
Wang S, Nath D, Chen W and Wang L 2020b Changes in winter stationary wave activity during weak mid-latitude and Arctic thermal contrast period *Int. J. Climatol.* **40** 1755–68
Woo S-H, Kim B-M, Jeong J-H, Kim S-J and Lim G-H 2012 Decadal changes in surface air temperature variability and cold surge characteristics over northeast Asia and their relation with the Arctic oscillation for the past three decades (1979–2011) *J. Geophys. Res. Atmos.* **117** D18117
Wu B 2017 Winter atmospheric circulation anomaly associated with recent Arctic winter warm anomalies *J. Clim.* **30** 8469–79
Wu B and Ding S 2023 Cold-Eurasia contributes to arctic warm anomalies *Clim. Dyn.* **60** 4157–72
Wu B, Li Z, Francis J A and Ding S 2022 A recent weakening of winter temperature association between Arctic and Asia *Environ. Res. Lett.* **17** 034030
Wu B, Su J and D'Arrigo R 2015 Patterns of Asian winter climate variability and links to Arctic Sea ice *J. Clim.* **28** 6841–58
Wu B, Su J and Zhang R 2011 Effects of autumn-winter Arctic sea ice on winter Siberian high *Chin. Sci. Bull.* **56** 3220–8
Wu B, Yang K and Francis J A 2017 A cold event in Asia during January–February 2012 and its possible association with Arctic Sea ice loss *J. Clim.* **30** 7971–90
Yao Y, Luo D, Dai A and Simmonds I 2017 Increased quasi stationarity and persistence of winter ural blocking and Eurasian extreme cold events in response to Arctic warming. Part I: insights from observational analyses *J. Clim.* **30** 3549–68
Yu Y, Xiao W, Zhang Z, Cheng X, Hui F and Zhao J 2021 Evaluation of 2-m air temperature and surface temperature from ERA5 and ERA-I using Buoy observations in the Arctic during 2010–2020 *Remote Sens.* **13** 2813
Zappa G, Ceppi P and Shepherd T G 2021 Eurasian cooling in response to Arctic sea-ice loss is not proved by maximum covariance analysis *Nat. Clim. Change* **11** 106–8
Zhang X, Lu C and Guan Z 2012 Weakened cyclones, intensified anticyclones and recent extreme cold winter weather events in Eurasia *Environ. Res. Lett.* **7** 044044
Zhang Y, Sperber K R and Boyle J S 1997 Climatology and interannual variation of the East Asian Winter Monsoon: Results from the 1979–95 NCEP/NCAR reanalysis *Mon. Wea. Rev.* **125** 2605–19